JURNAL REKAYASA PROSES
VOLUME 17, NUMBER 1, 2023, 49–59

RESEARCH ARTICLE

Optimization of low carbon steel coating with corrosion inhibitor method based on siwalan (Borassus flabellifer) fiber extract

Siti Khoirunnisa[1], Fawaid Syamsul Arifin[1], Nadia Erlina Mayangsari[1], Indra Setiawan[1], Evi Susanti[2,*]

[1]Department of Chemistry, Faculty of Mathematics and Sciences, Universitas Negeri Malang, Jl. Semarang 5, Malang 65145, Indonesia
[2]Department of Biology, Faculty of Mathematics and Sciences, Universitas Negeri malang, Jl. Semarang 5, Malang 65145, indonesia

Received 19 October 2021; revised 16 September 2022; accepted 21 October 2022

OBJECTIVES Siwalan fiber waste (SFW) has the potential as a source of lignin (7-25%) which is used as a green inhibitor to inhibit the corrosion rate of low carbon steel (LCS). The aims of this study were: (1) determine the optimum conditions (types of HCl and H_2SO_4, $C_{inhibitor}$ and C_{media}, inhibition temperature, and coating time) for LCS coating process using the inhibitory method using lignin extract from SFW, and (2) knowing the resistance of LCS coated with inhibitor at optimum conditions. METHODS Empirical research through laboratory experiments explains the relation between variables by analyzing numerical data. 185g of SFW produced 52.289g (28.26%) fine brown powder. RESULTS IR spectrum analysis on extract showed the wavelength was almost the same as the standard. IR spectrum analysis was also carried out on the extracted compounds that were adsorbed, and the absorption peaks confirmed the presence of lignin in the adsorbed compounds. CONCLUSIONS Based on the results of the analysis of the weighing data of the specimen before and after inhibition, the inhibitor concentration of 0.2–0.3 g/L in H_2SO_4 at 313K is the optimum condition to suppress the corrosion rate on the surface of LCS by 76.2%.

KEYWORDS corrosion inhibitor; corrosion rate; inhibition efficiency; lignin; siwalan fiber

1. INTRODUCTION

Straddling the equator, Indonesia is a tropical climate that produces endemic plant biodiversity, *Siwalan* (Borassus flabellifer). Based on data from the Department of Agriculture and Plantation of East Java Province in 2018, 93,000 - 186,000 tons of palm fiber waste were produced every day (Ministry of Agriculture Directorate General of Plantation, 2019). This leads to the accumulation of *siwalan* fiber waste in Indonesia because it is not used. On the other hand, *siwalan* fiber waste can be a source of lignin (7-25%) which can be treated as a green inhibitor for coating on low carbon steel, which reduces the corrosion rate (Dehghani et al. 2019). Reducing the corrosion rate will prevent technical accidents such as bridge collapses, building construction, and tank leaks at oil refineries, resulting in various financial losses, health, and death. (Alcántara et al. 2017).

Based on a research by Hassannejad and Nouri (2018), regarding lignin extract from sunflower seeds and Ramlah et al. (2020) with flavonoid extract from *beluntas* leaves, it has several shortcomings, namely the availability of sunflower seeds and *beluntas* leaves, which are not abundant in Indonesia and are widely used as food (Ramlah et al. 2020). It was found that the sunflower seed extraction research conducted by Hassannejad and Nouri (2018) only produced lignin extract of less than 8%, and the *beluntas* leaves only produced a corrosion rate inhibitory effect of only 2.31% (Farimani et al. 2020).

The results of the analysis regarding the application of lignin extract from *siwalan* fiber waste (Borassus flabellifer) in *LCS* have been carried out by Khoirunnisa Susanti et al. (2021) and demonstrated that the highest *LCS* resistance value is estimated to occur in the state of the optimization value of lignin inhibitor concentration in the range of 0.5 mg/day. 2.0-3,0 mg/L with immersion time ½ hours-24 hours on 0,5 M H_2SO_4 (Susanti et al. 2021). The results displayed that the lignin extract produced from *siwalan* fiber waste was predicted to have an inhibitory effect on the corrosion rate of up to 25.28% under conditions of optimum inhibitor concentration, temperature, and immersion time (Susanti et al. 2021).

*Correspondence: evi.susanti.fmipa@um.ac.id

Prof. Emeritus Dr. Carlton W. Dence mentioned that lignin has the potential as a corrosion inhibitor due to the presence of OH groups and aromatic rings in its structure as much as 82.71% (Divya et al. 2019). Thus, the objectives of this study are: (1) To find out the optimum conditions (types of HCl and H_2SO_4, inhibitor concentrations and acid media, inhibition temperature, and coating time) for the low carbon steel coating process using the inhibitory method using green inhibitor lignin extract of *siwalan* (*Borassus flabellifer*) fiber waste, and (2) Figuring out the percentage increase in the resistance of low carbon steel coated with green borer corrosion inhibitor at optimum conditions.

The significance of this research are: (1) The results of this study serve as a reference in dealing with corrosion rates in metals using the inhibition method and can provide a new source of literature in the development of science, especially in the field of local materials science in Indonesia, (2) The results of this research are the latest technological breakthroughs in overcoming the problem of the applicative resistance of *LCS* material to corrosive substances especially in Indonesia, (3) The results of this research provide innovations in a variety of inhibitor substances to provide solutions to prevent corrosion of metal materials, and (4) The use of *siwalan* fiber (locally fiber waste plant from Indonesia) can reduce waste that is not utilized, and optimize the use of abundant nature.

2. RESEARCH METHODOLOGY

This empirical research uses laboratory experiments to confirm the relationship between variables by analyzing the numerical data obtained. The independent variables of this study used variations of acid type, the concentration of inhibitor and acid (HCl and H_2SO_4), inhibition temperature, and coating time, with the control variable being *LCS* specimens

2.1 Materials

The materials needed are as follows: *siwalan* fiber waste dry in 100 mesh from Tuban East Java, *LCS* specimens (1 cm x 1.5 cm x 0.2 cm), 37% HCl, 98% H_2SO_4, NaOH p.a, technical acetone, and distilled water. The instrumentation needed are: sticky notes, grinder, analytical balance, universal pH indicator, thermometer, scissors, nylon thread, spray bottle, 70 mesh sieve, Whitman filter paper no. 1, 10 and 0.1 mL mohr pipettes, glass pipette, and stirrer, stand and clamp, Buchner funnel, oven, petri dish, 100 mL measuring flask, glass

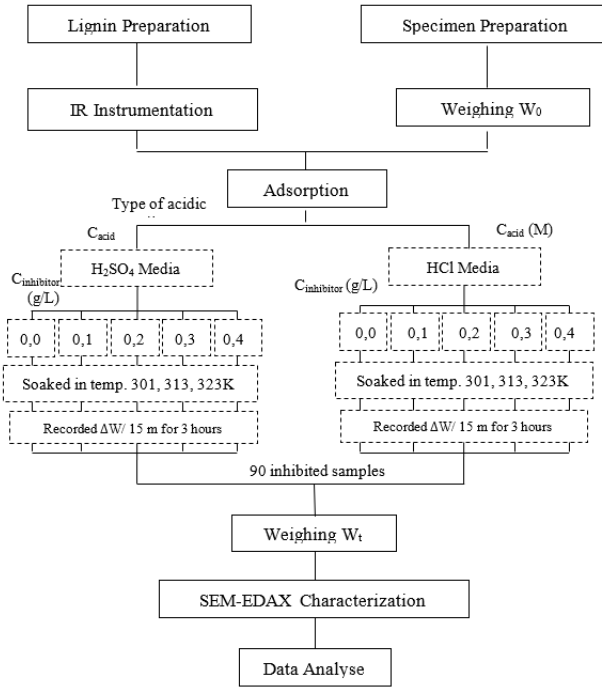

FIGURE 1. Research flowchart.

beaker and measuring cup, water bath, watch glass, desiccator, stainless spatula, and spoon, Shimadzu IR Prestige-21, SEM, and EDAX instruments

2.2 Research procedures

2.2.1 lignin preparation

The first step is to separate and clean the *siwalan,* and then after that, it is crushed and mashed. Then it is left in the oven to dry at 60°C for 24 hours. Next, the *siwalan* is dried, ground, and sieved. Furthermore, 185 grams of *siwalan* fiber powder was soaked in 2 L of 15% NaOH. The mixed solution was heated at 80°C and stirred for 6 hours. It was then left to be cooled to form a precipitate. The precipitate is separated from the filtrate. The filtrate was acidified with 40% H_2SO_4 to pH±2 and left for 1x24 hours to form a precipitate. The precipitate formed was filtered and dried in an oven at 60°C for 12 hours.

2.2.2 Specimen preparation

The specimen used is low carbon steel which has been cut with dimensions of 1 cm x 1.5 cm x 0.2 cm. After that, the spec-

TABLE 1. Sample code immersion in HCl with optimization of acidic concentration, inhibitors and temperature.

C_{acid}	Temp (K)	$C_{inhibitor}$ (g/L)				
		0.0	0.1	0.2	0.3	0.4
0.25 M	303	X01	A01	B01	C01	D01
	313	X02	A02	B02	C02	D02
	323	X03	A03	B03	C03	D03
0.5 M	303	X11	A11	B11	C11	D11
	313	X12	A12	B12	C12	D12
	323	X13	A13	B13	C13	D13
1.0 M	303	X21	A21	B21	C21	D21
	313	X22	A22	B22	C22	D22
	323	X23	A23	B23	C23	D23

TABLE 2. Sample code immersion in H_2SO_4 with optimization of acidic concentration, inhibitors, and temperature.

C_{acid}	Temp (K)	$C_{inhibitor}$ (g/L)				
		0,0	0,1	0,2	0,3	0,4
0,25 M	303	XX01	AA01	BB01	CC01	DD01
	313	XX02	AA02	BB02	CC02	DD02
	323	XX03	AA03	BB03	CC03	DD03
0,5 M	303	XX11	AA11	BB11	CC11	DD11
	313	XX12	AA12	BB12	CC12	DD12
	323	XX13	AA13	BB13	CC13	DD13
1,0 M	303	XX21	AA21	BB21	CC21	DD21
	313	XX22	AA22	BB22	CC22	DD22
	323	XX23	AA23	BB23	CC23	DD23

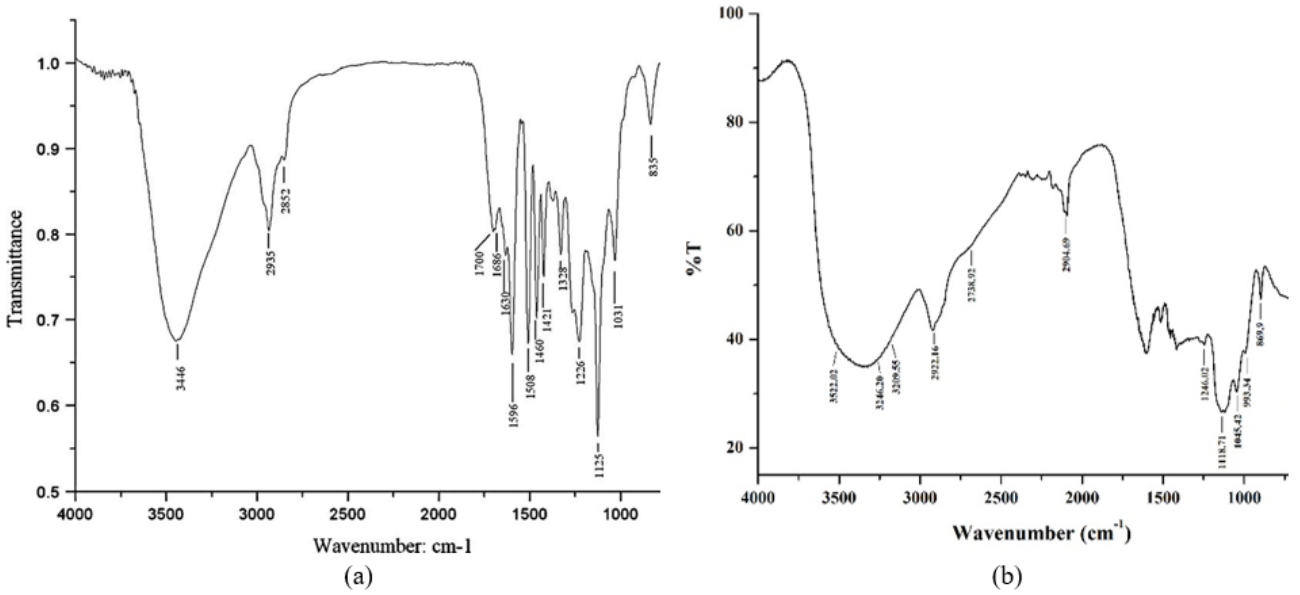

FIGURE 2. IR spectra of (a) standard lignin and (b) compound extract.

imens were sanded. Sanding is done in 2 steps, the first is sanding with 80 grit to remove the plating that sticks to the specimen surface, and then sanding with 150 grit to smooth the surface that has been clean from the plate so that it has a homogeneous surface. After sanding, specimen cleaned with distilled aquadest to rinse off the remaining sandpaper. After rinsed by aquadest, specimen rinsed with acetone, and then dried in an oven at 60°C for 10 minutes. The dry sample was then cooled and then weighed (W_0).

2.2.3 Lignin adsorption process on LCS specimens

Specimens with known initial weight (W_0) was immersed in an acid solution (HCl and H_2SO_4) with a concentration variation of 0.25; 0.5; and 1M for 2 hours (recorded mass every 15 minutes and dried for ± 3 minutes). Then the specimen was washed with distilled water, rinsed with acetone, dried in an oven at 60°C for 15 minutes, then weighed the final mass of the whole process (W_t).

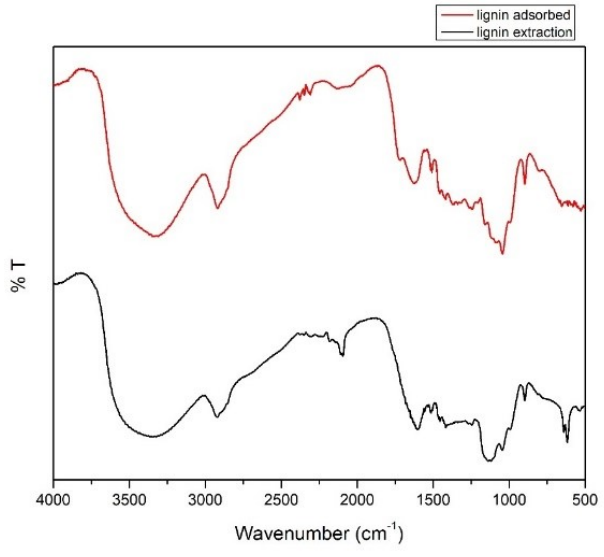

FIGURE 3. IR spectra of adsorbed lignin compounds.

2.2.4 Data collection

The results of LCS mass weighed before, during, and after the inhibition were recorded and tabulated with sample codes presented in Tables 1 and 2.

2.3 Instrument and data analysis

2.3.1 Characterization of lignin functional groups using FTIR

The extracted lignin in solid/powder was tested to determine the functional groups of lignin compounds using FTIR. Sample preparation (for solid samples, the sample is mixed with KBr in a ratio of 1:10 and for the sample it must be free of H_2O and placed between 2 KBr plates) then analysis is carried out. Identification of functional groups was analyzed by observing the absorption peaks that appear at specific wavelengths and compared based on standard absorption references.

2.3.2 Microscopic characterization of specimens using SEM and EDAX

LCS specimens before and after adsorption with and without the addition of lignin inhibitors were characterized to examine their pore size and confirmed the presence of lignin constituents on the surface of the adsorbed specimen. The sample to be analyzed is placed in a holder measuring ± 10mm. the sample was prepared by coating using Au-Pd (this aims to make the sample more conductive). The sample is put into the SEM chamber then low vacuum pump. Characterization results were compared between specimens before inhibited, uninhibited, and after inhabited by lignin.

2.3.3 Data analysis and interpretation

In order to analyze the data, quantitative descriptive analysis is employed to help summarize the results and calculating the inhibition efficiency and the effectiveness of reducing the corrosion rate. Data is interpreted into tables and histograms.

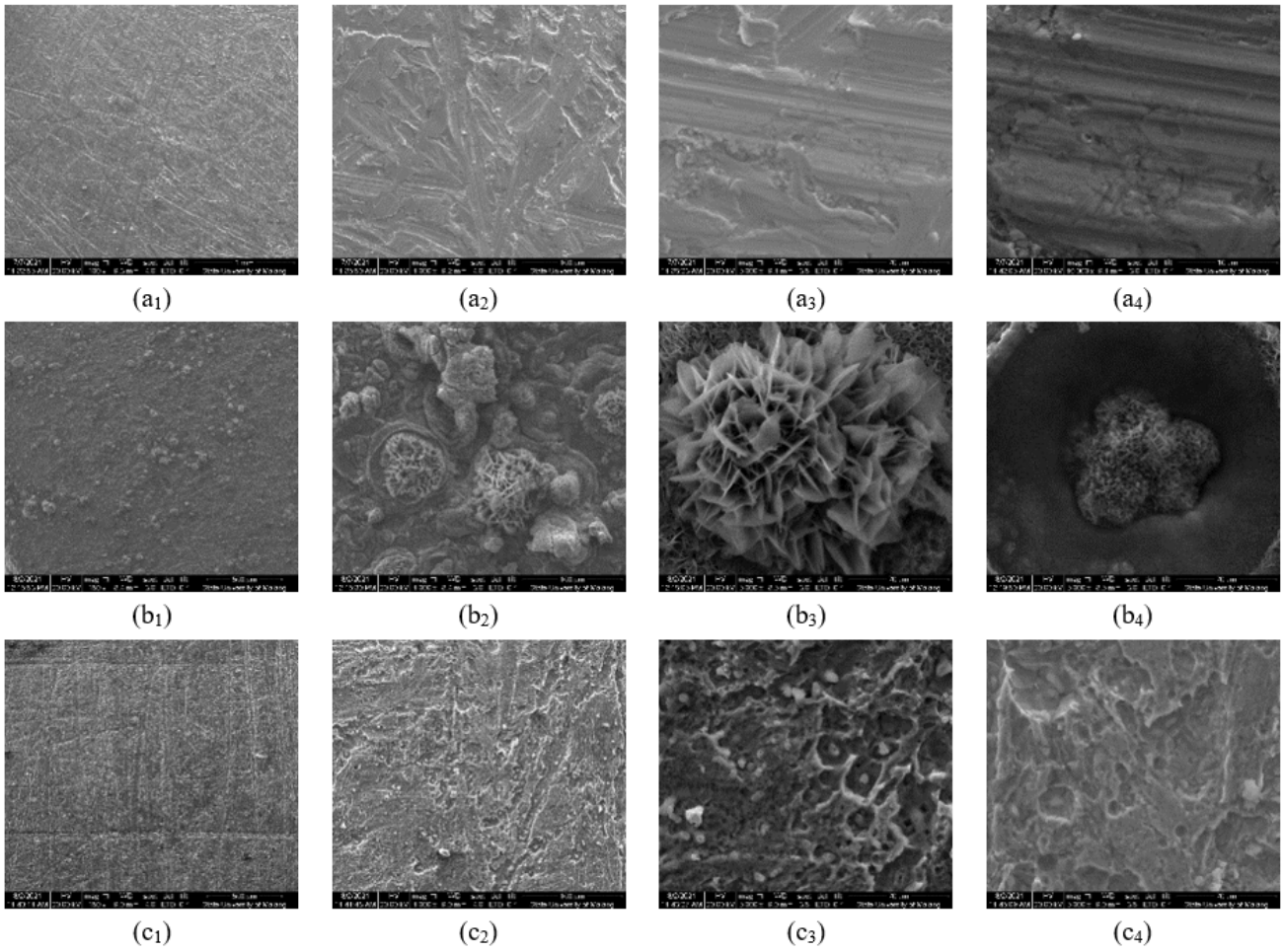

FIGURE 4. SEM of low carbon steel specimens: (a) before inhibition, (b) after inhibition without inhibitor, (c) after inhibition with inhibitor.

2.3.4 Percentage of lignin extract yield from siwalan fiber

The yield of lignin resulting from the extraction of *siwalan* fibers is calculated using the equation1.

$$\text{Extract Yield Lignin}(\%) = \frac{\text{weight of extracted lignin}}{\text{weight of siwalan fiber}} \times 100\% \quad (1)$$

2.3.5 Calculation of the weight loss measurement and method of calculation of inhibition efficiency

The test using the weight loss method refers to the ASTM G31-72 standard. The inhibited low carbon steel specimens were then weighed, and the percentage of inhibition efficiency and corrosion rate was determined.

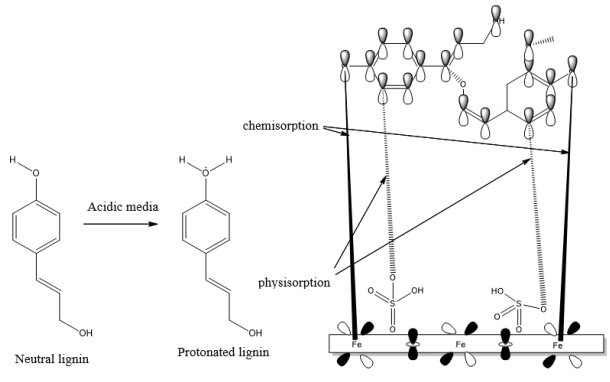

FIGURE 5. Inhibitor adsorption mechanism on Fe surface.

2.4 Stage of research

Figure 1 is the stage of the research carried out. The data analysis technique used was quantitative descriptive analysis by summarizing the research results, calculating the % efficiency of corrosion inhibition and reduction, interpretation of IR spectrum data, and analysis of microscopic morphology and compound content in the specimen using SEM-EDAX.

3. RESULTS AND DISCUSSION

3.1 Lignin extract yield

The *siwalan* fiber used as the material for this research was obtained from Tuban, East Java district. The extract obtained from 185 grams of *siwalan* fiber waste produced 52.289 grams (28.26%) of fine brown powder. Based on Figure 2 (b), the presence of several functional groups contained in compounds extracted from *siwalan* fiber waste such as phenolic O–H groups at a wavelength of 3522.02 and a sharp peak at a wavelength of 3209.55 cm^{-1} indicates the presence of O–H groups. This functions as a center for the adsorption of inhibitors. At wavelengths 1246.02 and 1118.71 cm^{-1} indicated a bending vibration of the alcohol C–O group and 993.34 cm^{-1}, which indicated the presence of an aliphatic C=H group. The absorption peaks have almost the same wavelength as Figure 2. (a) as the standard IR spectrum of lignin (alkali) (web-

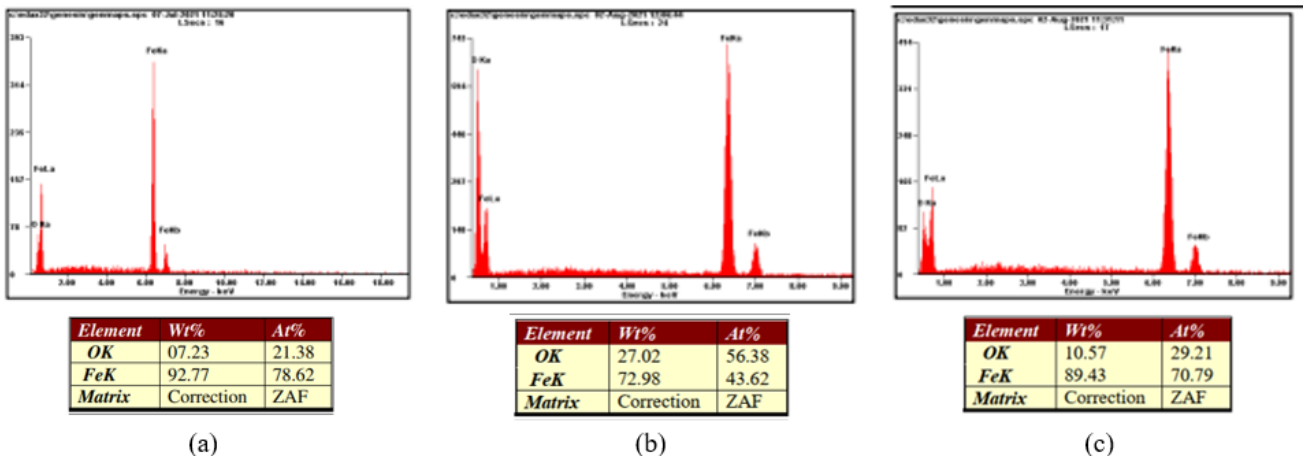

Element	Wt%	At%
OK	07.23	21.38
FeK	92.77	78.62
Matrix	Correction	ZAF

(a)

Element	Wt%	At%
OK	27.02	56.38
FeK	72.98	43.62
Matrix	Correction	ZAF

(b)

Element	Wt%	At%
OK	10.57	29.21
FeK	89.43	70.79
Matrix	Correction	ZAF

(c)

FIGURE 6. EDAX test results of low carbon steel specimens: (a) before inhibition, (b) after inhibition without inhibitor in AA01, (c) after inhibition with inhibitor in BB01 sample.

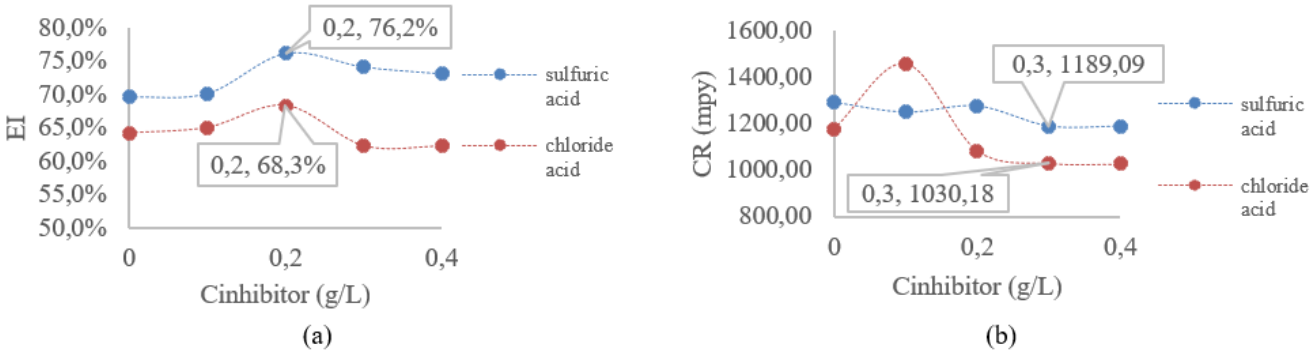

FIGURE 7. Graph of the effect of lignin concentration on (a) inhibition efficiency, (b) corrosion rate.

book.nist.gov). It is analyzed and confirmed that the compound obtained was a lignin compound. The IR spectrum of standard lignin has a narrower peak, on the other hand, the compound extract has a wider peak because it describes a bond that includes a lot of energy. The widening is because the intermolecular H-bonding shows a widening of the IR band due to the strength of the continuum bond.

3.2 Adsorbed lignin compound

The FT-IR test was also carried out on the solid brown coating the specimen to confirm the formation of new compounds after the inhibition process. Figure 3 is the IR spectrum of the extracted compound adsorbed on the specimen. The absorption peaks at wavelengths 3487.3, 1612.49, 1508.33, 1373.32, and 10423 cm^{-1} respectively indicate the presence of stretching vibrations of phenolic OH groups, aromatic C=C, OH bending vibrations in the plane, and the stretching vibration of the aromatic ring CO which confirmed the presence of lignin content in the adsorbed compound. The fingerprint region shows a complex bond between the specimen and the extracted compound, which was adsorbed were Fe-O at the wavelength of 653,87 cm^{-1} and corrosion products β-FeOOH and β-Fe_3O_4 at wavelength 804,32, dan 896,9 cm^{-1}.

3.3 SEM and EDAX microscopic analysis

SEM-EDAX characterization was carried out on low carbon steel specimens before inhibition and inhibited specimens in HCl and H_2SO_4 media with and without inhibitors at 100x,

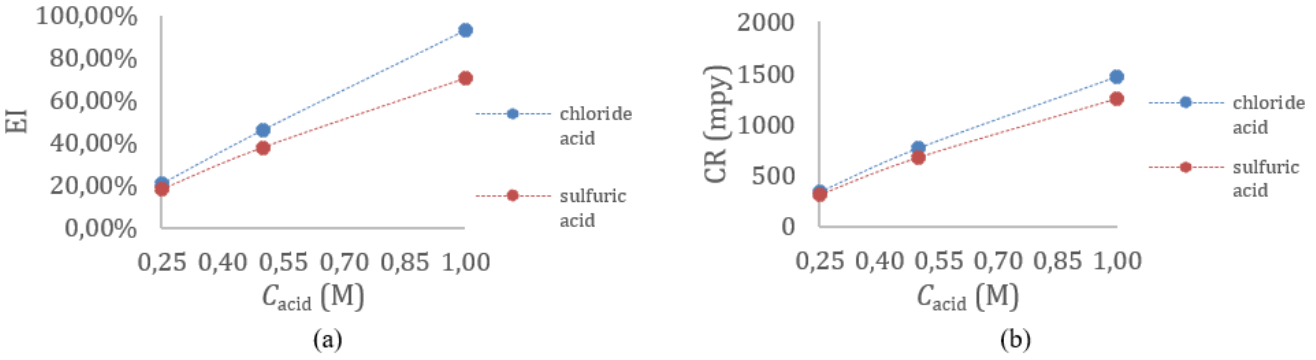

FIGURE 8. Graph of the effect of acid concentration on (a) inhibition efficiency, (b) corrosion rate.

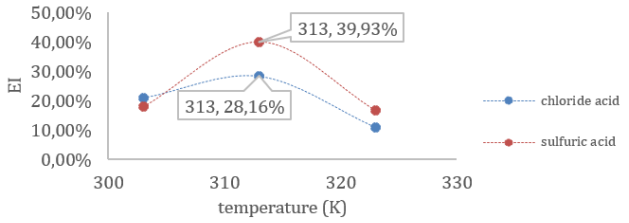

FIGURE 9. Graph of the effect of temperature on inhibition efficiency.

1000x, 5000x, and 10000x magnifications. Figure 4 (a) illustrated the condition of the specimen before the inhibition process, which demonstrated that holes and cracks had not yet formed. Figure 4 At 1000x magnification, clusters of various sizes on the specimen after inhibition are spread over almost every surface. 1000x magnification Figure 4. (b_2) and (c_2) clusters were formed in both specimens, but more clusters were formed in the specimens without inhibitor, almost evenly on the surface and 38.971µm larger than the specimens using 2.168 m inhibitors. At 5000x magnification, as shown in Figures 4 (b_3) and (c_3), the holes formed in the specimen without the inhibitor are almost uniformed on the surface and are larger than the holes in the specimen with the inhibitor on the uneven surface (Mobin et al. 2019). While at 10000x magnification in Figure 4 (b_4) and (c_4), cracks are seen in both specimens. Specimens without inhibitors had more cracks than those with inhibitors.

Lignin compounds consisting of monomers p-coumaryl-, coniferyl-, and sinapyl alcohol have the potential as corrosion inhibitors on metals. This makes lignin compounds potential as centers of adsorption inhibitors and can inhibit the rate of corrosion. The inhibition of corrosion rate of low carbon steel (LCS) in H_2SO_4 by neutral and protonated monolignol lignin was explained based on molecular adsorption. Lignin monolignol inhibitors are predicted to be adsorbed on the LCS surface in the following manner:

1. Donor-acceptor interaction between the π electron of the aromatic ring of the inhibitor species and the vacant d orbital of the iron atom on the surface,
2. The interaction between the lone pair of heteroatoms of the neutral inhibitor and the unpaired electrons of the protonated inhibitor with the empty d orbitals of the iron atom on the surface of the LCS.

Based on the MD simulation and MC calculation results thant have been conduct by Susanti et al. (2021), two interactive simulations can be predicted during the adsorption process. Neutral and protonated species of lignin compounds interact with sulfate ions previously adsorbed on the surface of the LCS, resulting in the physisorption of inhibitor molecules. With this, the inhibitor molecule competes with the H^+ proton of sulfuric acid to form bonds with the electrons of Fe atoms on the surface of the LCS, however, based on the plot calculation data E_{HOMO} and E_{LUMO}, protonated lignin compounds more easily form bonds with Fe atoms than protons H^+.

Corrosion inhibitor species are adsorbed on the surface of the LCS through a chemisorption mechanism that involves the transfer of electrons from the inhibitor heteroatom to the Fe atom on the surface of the LCS in sulfuric acid media. Inhibitor molecules can also be adsorbed on the surface of LCS based on donor-acceptor interactions between electrons π from the heterocyclic ring to the empty *d* orbital of the surface iron. The corrosion inhibition mechanism is shown in Figure 5.

Cracks and holes formed are the main factors causing corrosion because they are the entrance for corrosive substances to oxidize iron on the surface of low carbon steel (Nathiya et al. 2019; Shi et al. 2018). The results of the EDAX test on specimens without and with inhibitors are shown in Figures 6 (b) and (c). The test results are compared with Figure 6 (a), which is the result of the EDAX test of the specimen before inhibition.

Based on the results of the EDAX test in before and after inhibition with and without inhibitor. EDAX test sample used in optimum condition specimenwhich is AA01 ($C_{inhibitor}$ 0 g/ 0.25 M in H_2SO_4) and BB01 specimen ($C_{inhibitor}$ 0.2 g/ 0.25 M in H_2SO_4). The specimens before inhibition showed the per-

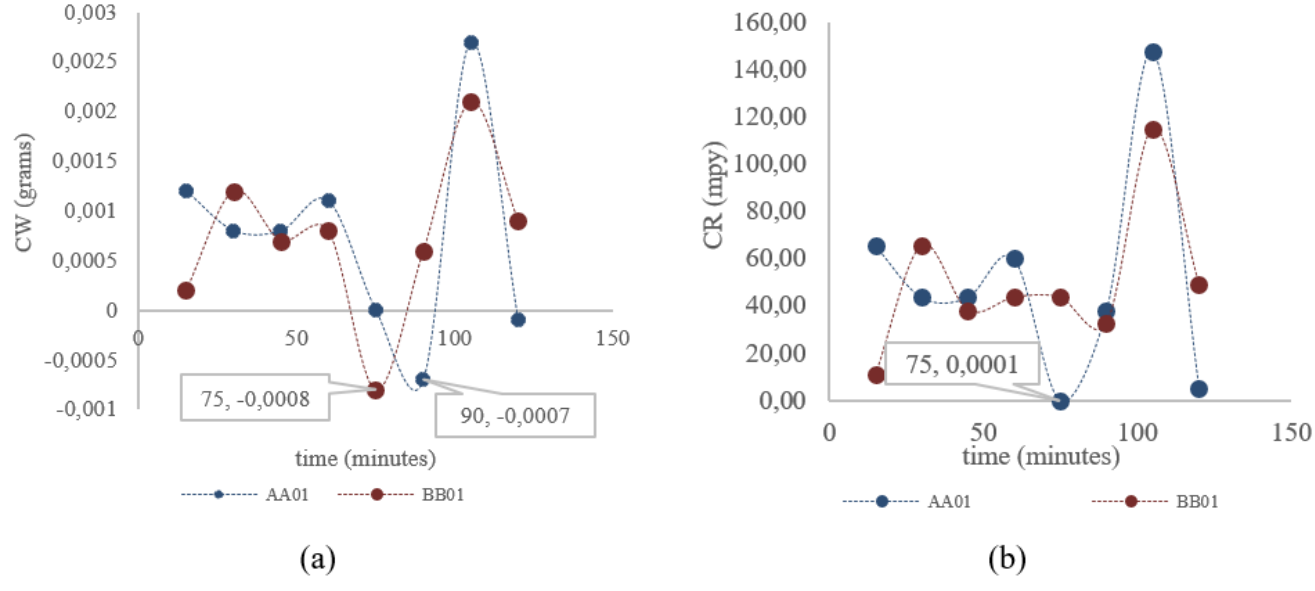

FIGURE 10. Graph of the effect of immersion time on (a) changes in weight, (b) corrosion rate.

TABLE 3. Prediction of quantum chemical calculations for the neutral and protonated p-coumaryl-, coniferyl-, and sinapyl alcohol compounds DFT/B3LYP base set 6-31G(d,p).

	E_{HOMO}	E_{LUMO}	ΔE (eV)	PI (eV)	ΔN	AE (eV)	χ (eV)	η
p-coumaryl neutral	-0.02354	-0.20255	0.17901	0.02354	-0.49267	0.20255	-0.11305	0.08951
p-coumaryl protonated	-0.19024	-0.34956	0.15932	0.19024	1.31824	0.34956	-0.26990	0.07966
coniferyl neutral	-0.02389	-0.20156	0.17767	0.02389	-0.50251	0.20156	-0.11273	0.08884
coniferyl protonated	-0.16930	-0.34146	0.17216	0.16930	0.98406	0.34146	-0.25538	0.08608
sinapyl neutral	-0.02294	-0.19418	0.17124	0.02294	-0.58188	0.19418	-0.10856	0.08562
sinapyl protonated	-0.15673	-0.33420	0.17747	0.15673	0.83176	0.33420	-0.24547	0.08874

centage of Fe elements of 92.77% and O 7.23%, while in the specimens after initiation without inhibitors, the Fe content was only 72.98%, and 27.02% of O elements formed due to acid reactions with the specimen in the inhibition process. Based on Figure 6. the percentage of elemental O content without inhibitor is more than with inhibitor (10.57%); this indicates an inhibitory effect on the formation of corrosion products (Fouda et al. 2016).

3.4 Calculation results of corrosion rate and corrosion rate inhibition effect

Based on the results of weighing the specimens before and after inhibition in HCl and H_2SO_4 media, data analysis can be carried out to determine the effect of independent variables on the optimum control of low carbon steel resistance (Pradityana et al. 2013).

3.5 Effect of lignin concentration on inhibition efficiency and corrosion rate

The calculation of the efficiency of inhibition and corrosion rate of steel in HCl and H_2SO_4 0.25M media with and without inhibitors of *siwalan* fiber waste extract under immersion for 2 hours at 303K is shown in Figure 7 (a) and (b), respectively. Based on Figure 7. (a) shows that the concentration of the inhibitor compound extract (lignin) varied, while Figure (b) shows that the greater the concentration of inhibitor (lignin) used, the lower the corrosion rate, both in HCl and H_2SO_4 media. This is because the adsorbed extract compounds bind to the iron to form a thin layer that protects the specimen from corrosive substances (Ahanotu et al. 2020). The inhibitor concentration of 0.2 – 0.3 g/L in HCl and H_2SO_4 is the highest optimization of the addition of inhibitors to achieve the percent inhibition efficiency and optimum corrosion rate.

3.6 The effect of acid concentration on inhibition efficiency and corrosion rate

The results of the calculation of the efficiency of inhibition and corrosion rate of steel in HCl and H_2SO_4 at concentrations of 0.25, 0.50, 1.00M with and without inhibitors of siwalan fiber waste extract under immersion in 2 hours at 303K are shown in Figure 8 (a) and (b).

Based on Figure 8 (a), the higher the acid concentration, the higher the percentage of inhibition efficiency. Figure 8 (b) also shows that the greater the acid concentration used, the higher the corrosion rate, both in HCl and H_2SO_4 media. This is because high acid concentration and inhibitor adsorption process causes the iron on the low carbon steel surface to be oxidized and result in corrosion (Alibakhshi et al. 2019). However, the graph of the increase in the corrosion rate, which is more sloping than the percentage value of the inhibition efficiency, shows that the optimization of the function of the acid as an inhibitor adsorption medium is more substantial (Hassannejad and Nouri 2018). The type of acid used also affects the percentage of inhibition efficiency and corrosion rate. Hydrochloric acid (HCl) has a higher percentage of inhibition efficiency than sulfuric acid (H_2SO_4). This is because HCl is a strong acid that is more stable than sulfuric acid with high reactivity (Haddadi et al. 2019).

3.7 The effect of temperature on inhibition efficiency

The graph displaying the relationship between temperature and the calculation of the percent inhibition efficiency in HCl and H_2SO_4 is shown in Figure 9. Figure 9 displays the percentage optimization of the highest inhibition efficiency at 313K in HCl and H_2SO_4 media, 28.16 and 39.93%, respectively.

3.8 The effect of immersion time on changes in weight and corrosion rate

The graph illustrating the relationship between immersion time on changes in specimen weight and corrosion rate in 0.25M HCl and H_2SO_4 are presented in Figure 10. (a) and (b), respectively. Based on Figure 10. (a) shows the length of immersion time (inhibition process), which varies with the influence of changes in specimen weight (ΔW). This is caused by the formation of corrosion products that make the specimen porous during the inhibition process. In the 75^{th} to 90^{th} minute, there was an increase in the weight of the specimen, which was indicated by a negative value of W. This is due to

TABLE 4. The inhibition efficiency (IE%) for neutral and protonated p-coumaryl, coniferyl, and sinapyl alcohol compounds.

Compound	$PI_{inhibitor}$	$E_{HOMO\ inhibitor\text{-}Fe}$	$PI_{inhibitor\text{-}Fe}$	PI_{add}%	$IE_{add.}$	Inhibition Efficiency (%)	
						Theory	Experiment
p-coumaryl alcohol	0.02354	-0.49174	0.49174	23.4100	4.7400	23.4100	18,67
p-coumaryl alcohol protonated	0.19024	-0.65282	0.65282	23.1290	4.4590	23.1290	—— ——
coniferyl alcohol	0.02389	-0.47881	0.47881	22.7460	4.0760	22.7460	—— ——
coniferyl alcohol protonated	0.16930	-0.61238	0.61238	22.1540	3.4840	22.1540	—— ——
sinapyl alcohol	0.02294	-0.47482	0.47482	22.5940	3.9240	22.5940	—— ——
sinapyl alcohol protonated	0.15673	-0.59390	0.59390	21.8585	3.1885	21.8585	—— ——

 DOI 10.22146/jrekpros.69851

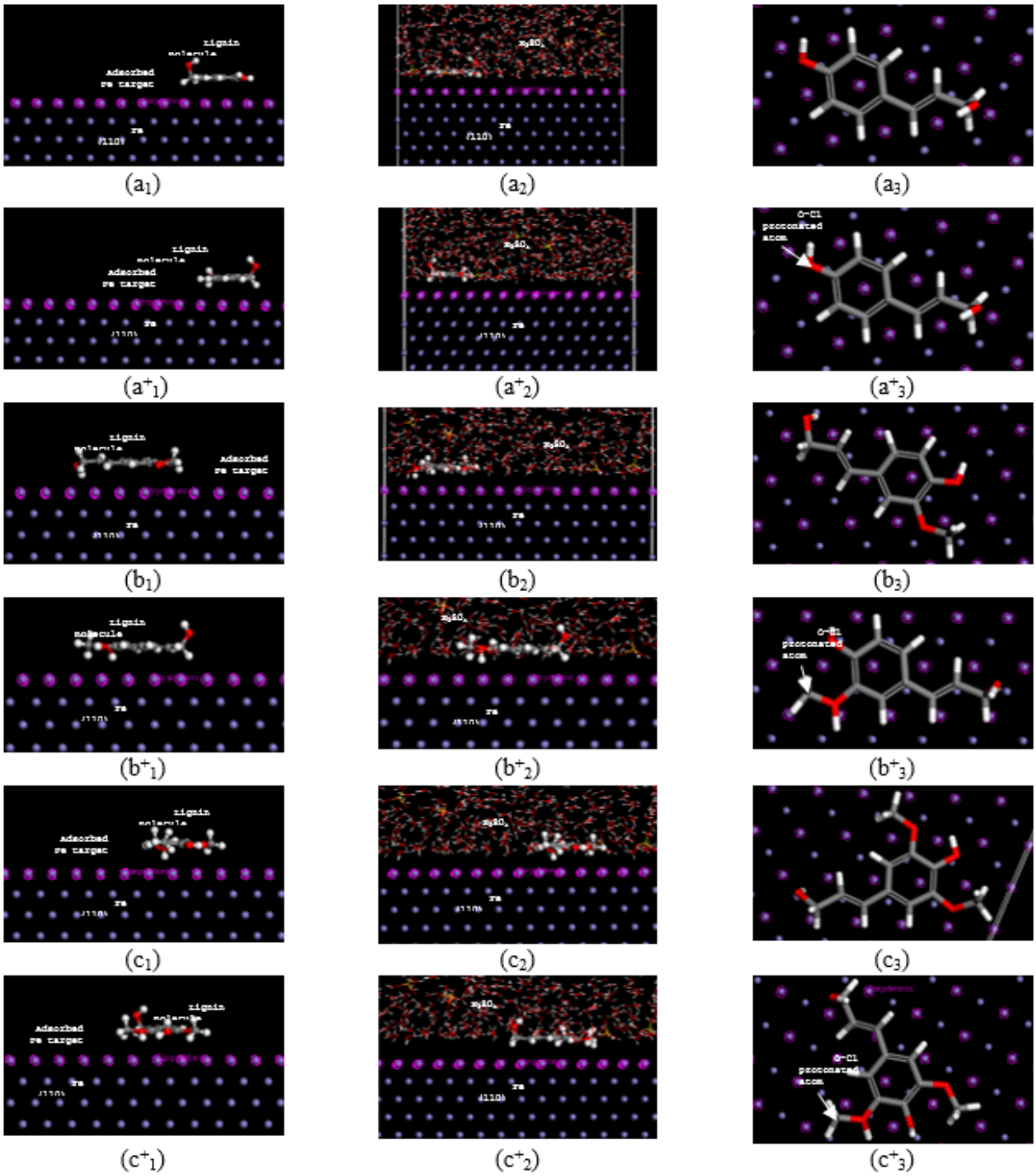

FIGURE 11. Adsorption simulation of monolignol lignin (a) p-coumaryl-, (b) coniferyl-, and (c) sinapyl alcohol on Fe (110).

the presence of inhibitors adsorbed on the surface of low carbon steel (Rosli et al. 2019). The difference in the acid concentrations used also influences the weight loss of the specimen. Figure 10 (a) shows that H_2SO_4 experienced a significant change in the weight of the specimen. This event is because H_2SO_4 oxidizes iron strongly and adsorbs corrosion inhibitors rather than HCl. While in Figure 10 (b) is a graph of the effect of immersion time on the corrosion rate. The graph shows at 75th minute in H_2SO_4 media, which is the optimum condition to suppress the corrosion rate on the surface of low carbon steel.

4. ADDITIONAL DATA

4.1 Reactivity of Lignin Species as Corrosion Inhibitor

From a previous literature review, it is acknowledged that the value of the transferred electron fraction (ΔN), which is higher than zero (positive value), indicates the fact that the inhibitor molecule can transfer its electrons to Fe atoms on the surface of the LCS. However, if the value of this parameter is lower than zero, it proves the existence of electron transfer derives from the metal to the inhibitor. The data collected in table 1 explained that if N's value for neutral and protonated inhibitors is positive, it indicates that all neutral

TABLE 5. The inhibition efficiency (IE%) for neutral and protonated p-coumaryl, coniferyl, and sinapyl alcohol compounds.

Compound	$E_{inhibitor}$	$E_{inhibitor\ (acid)}$	E_{total}	E_{add} (without acid)	E_{add} (acid)	$E_{bonding}$ (acid)
p-coumaryl alcohol	-12,312	8,846	-7258,304	-54,314	-73,998	73,998
p-coumaryl alcohol protonated	-21,743	9,844	-7267,284	-44,381	-83,976	83,976
coniferyl alcohol	7,275	12,366	-7245,910	-35,931	-65,124	65,124
coniferyl alcohol protonated	1,288	12,458	-7250,970	-40,973	-70,276	70,276
sinapyl alcohol	19,673	18,783	-7239,836	-35,921	-65,467	65,467
sinapyl alcohol protonated	18,503	15,279	-7239,905	-32,321	-62,032	62,032

and protonated lignin molecules tend to donate electrons to empty orbitals of Fe atoms. The highest PI value explained that the molecule had the highest adsorption reactivity as a corrosion inhibitor. Table 3. shows the pattern of increasing the value of the ionization potential, which is correlated with the pattern of increase in E_{HOMO}. Based on equation 3, the PI value is obtained from the negative value E_{HOMO}. The PI of the protonated p-coumaryl alcohol compound is 0.19024 eV, the highest among the ionization potential values of other compounds. This proves that the highest adsorption reactivity is in the protonated monolignol lignin compound p-coumaryl alcohol.

Moreover, Table 3. also indicates the value of the difference in electronegativity of each neutral and protonated monolignol lignin molecule. The value of a slight difference in electronegativity in a molecule indicates that the molecule tends to reach electron equilibrium, making the molecule less reactive than other molecules and vice versa. This signifies that protonated p-coumaryl alcohol compounds are in a very reactive condition as corrosion inhibitors. Protonated p-coumaryl alcohol compounds are more easily bound to Fe atoms on the surface of LCS to achieve electron distribution equilibrium than other compounds.

Table 4 exhibited the results of the calculation of the inhibition efficiency (IE_{theory}%) of neutral and protonated p-coumaryl-, coniferyl-, and sinapyl alcohol compounds. The data showed irregular %IE values in each analyzed lignin molecule. The calculation results explain that adding electron donor groups such as hydroxyl and methoxy groups to the inhibitor compound may not necessarily increase the percentage of inhibition efficiency. Based on the data in Table 4. and according to the results of the pattern calculation E_{HOMO}, ionization potential, and electronegativity can be predicted that the p-coumaryl alcohol molecule has the highest inhibition efficiency value of 23.4100% compared to other compounds. This is because the donor-acceptor interaction between the electrons of the aromatic ring and the lone pair of inhibitor heteroatoms with the empty d orbital of the iron atom on the surface of the LCS is stable on the phenolic group, causing the p-coumaryl alcohol molecule bound to the Fe atom to be more stable than other molecules.

4.2 Absorptivity of Fe Atoms on the Surface of LCS in H_2SO_4

The interfacial adsorption of monolignol lignin compounds (p-coumaryl-, coniferyl-, and neutral and protonated sinapyl alcohol) on the surface of the Fe(110) target was theoretically simulated using a combination of Monte Carlo (MC) calculations and Molecular Dynamic (MD) modeling. The graphical results of the MD modeling are visualized in Figure 11. The side view proves that the protonated and neutral p-coumaryl, coniferyl, and sinapyl alcohol molecules tend to approach the crystallographic plane of Fe (110).

The top vertical cross-section view of the resulting graphic Figure 11 demonstrates molecules' adsorption in a flat frame orientation. The lignin molecule has a larger size than the Fe atom so that the predicted bond does not occur at the junction of the iron crystals. This can cause a steric effect on the monolignol lignin molecule, but based on the results of the MC calculation, the molecule will be adsorbed on the Fe surface and form an absorbent layer with solid chemical bonds that the iron element does not undergo direct contact with corrosive substances. The results of the MC calculation explained that the optimization of the highest negative value of adsorption energy was in the condition of 0.50M H_2SO_4 media with an inhibition temperature of 303K. This explains that the 0.50M H_2SO_4 medium with an inhibition temperature of 303K is the optimum condition for the inhibitor adsorption process, which is characterized by the largest binding energy value among other control conditions. Table 5 is the MC optimization data at optimum conditions. The quantitative results of the respective MC simulations showing the calculation of the adsorption energies of the neutral and protonated p-coumaryl-, coniferyl-, and synapyl alcohol molecules.

Based on the data in Table 5, the adsorption energy of p-coumaryl-, coniferyl-, and sinapyl alcohol molecules, both neutral and protonated, presents a negative value of adsorption energy. This indicates the tendency of monolignol lignin molecules to bind to Fe atoms on the surface of the LCS. The ease of adsorption of neutral and protonated monolignol lignin molecules occurs when the molecules that make up the media (H_2O, HSO_4^-, and H^+) are at the interface, this is because the added H_2SO_4 media functions as an oxidizer on the target iron surface which can facilitate the adsorption process of neutral and protonated monolignol lignin molecules. In addition, the results of the MC calculation of predicted molecules in H_2SO_4 media also show that protonated p-coumaryl alcohol molecules have the highest negative adsorption energy value compared to other molecules. The negative value of the greater adsorption energy indicates that the value of the binding energy of the molecule is increasingly positive. The positive value of the binding energy of the inhibitor molecule indicates the bond strength of neutral and protonated monolignol lignin compounds adsorbed on Fe LCS. The protonated p-coumaryl alcohol molecule has the highest binding energy, indicating that the molecule has the strongest bond (chemisorption) with Fe atoms compared to other molecules.

4.3 The Effect of H_2SO_4 as an Inhibitory Adsorption Media on Iron Atoms on the Surface of LCS

The result of the MC calculation shows that the enthalpy of Fe-inhibitor is 19.673 kcal/mol, while Fe-acid is -126.082 kcal/mol. A negative enthalpy indicates that the bond energy being broken is greater than the binding energy formed. The enthalpy value of the Fe atom bonded to the sulfate anion is negative, which indicates that the binding energy between the broken Fe atoms is greater than the binding energy of the Fe-acid formed (it is difficult to form a product). The binding energy between Fe atoms is smaller than the binding energy of the Fe-inhibitor formed, which causes the acid to function as a medium for adsorption of lignin molecules on Fe atoms. The MC calculations proved that the adsorption energy of inhibitor molecules in sulfuric acid media is more negative than without sulfuric acid; this more negative value signifies how easily inhibitor molecules are adsorbed on Fe atoms on the surface of the LCS.

5. CONCLUSIONS

Based on the research that has been done, *siwalan* fiber waste produces 28.26% of fine brown powder. The results of the IR spectrum analysis on the extract confirms that the extraction compound obtained is a lignin compound. The analysis of the IR spectrum presented that indicated presence of lignin compounds in the adsorbed compounds. The results of the SEM test at 1000x magnification showed the presence of an inhibitor can hinder the formation of corrosion products in the specimen. At 5000x magnification, the holes formed in the specimen without the inhibitor are almost uniform on the surface than the holes in the specimen with the inhibitor, which are uneven. At 10000x magnification, cracks occur in both specimens. Specimens without inhibitors had more cracks than those with inhibitors. This is the main factor causing corrosion. Based on the results of the analysis of the data weighing specimens before and after inhibition showed: a) The condition of the inhibitor concentration of 0.2 – 0.3 g/L in HCl and H_2SO_4 was the highest optimization of the addition of inhibitors to achieve the percent inhibition efficiency and optimum corrosion rate; b) the graph of the increase in the corrosion rate which is more sloping than the percentage value of the inhibition efficiency shows the optimization of the function of the acid as a stronger inhibitor adsorption medium; c) the effect of temperature on inhibition efficiency showed that the highest percentage optimization of inhibition efficiency was at a temperature of 313K in HCl and H_2SO_4, which were 28.16 and 39.93%, respectively; d) at 75^{th} minute in H_2SO_4, as the optimum condition to suppress the corrosion rate on the surface of low carbon steel.

6. ACKNOWLEDGEMENTS

A deep sense of gratitude to the Universitas Negeri Malang and the Ministry of Education, Culture, Research, and Technology for funding the implementation of PKM-Exact Research.

REFERENCES

Ahanotu CC, Onyeachu IB, Solomon MM, Chikwe IS, Chikwe OB, Eziukwu CA. 2020. Pterocarpus santalinoides leaves extract as a sustainable and potent inhibitor for low carbon steel in a simulated pickling medium. Sustainable Chemistry and Pharmacy. 15:100196. doi:10.1016/j.scp.2019.100196.

Alcántara J, de la Fuente D, Chico B, Simancas J, Díaz I, Morcillo M. 2017. Marine atmospheric corrosion of carbon steel: A review. Materials. 10(4). doi:10.3390/ma10040406.

Alibakhshi E, Ramezanzadeh M, Haddadi SA, Bahlakeh G, Ramezanzadeh B, Mahdavian M. 2019. Persian Liquorice extract as a highly efficient sustainable corrosion inhibitor for mild steel in sodium chloride solution. Journal of Cleaner Production. 210:660–672. doi:10.1016/j.jclepro.2018.11.053.

Dehghani A, Bahlakeh G, Ramezanzadeh B. 2019. Green Eucalyptus leaf extract: A potent source of bio-active corrosion inhibitors for mild steel. Bioelectrochemistry. 130:107339. doi:10.1016/j.bioelechem.2019.107339.

Divya P, Subhashini S, Prithiba A, Rajalakshmi R. 2019. Tithonia diversifolia flower extract as green corrosion inhibitor for mild steel in acid medium. Materials Today: Proceedings. 18:1581–1591. doi:10.1016/j.matpr.2019.05.252.

Farimani AM, Hassannejad H, Nouri A, Barati A. 2020. Using oral penicillin as a novel environmentally friendly corrosion inhibitor for low carbon steel in an environment containing hydrogen sulfide corrosive gas. Journal of Natural Gas Science and Engineering. 77:103262. doi:10.1016/j.jngse.2020.103262.

Fouda AS, Shalabi K, E-Hossiany A. 2016. Moxifloxacin antibiotic as green corrosion inhibitor for carbon steel in 1 M HCl. Journal of Bio- and Tribo-Corrosion. 2(3). doi:10.1007/s40735-016-0048-x.

Haddadi SA, Alibakhshi E, Bahlakeh G, Ramezanzadeh B, Mahdavian M. 2019. A detailed atomic level computational and electrochemical exploration of the Juglans regia green fruit shell extract as a sustainable and highly efficient green corrosion inhibitor for mild steel in 3.5 wt-NaCl solution. Journal of Molecular Liquids. 284:682–699. doi:10.1016/j.molliq.2019.04.045.

Hassannejad H, Nouri A. 2018. Sunflower seed hull extract as a novel green corrosion inhibitor for mild steel in HCl solution. Journal of Molecular Liquids. 254:377–382. doi:10.1016/j.molliq.2018.01.142.

Mobin M, Basik M, Aslam J. 2019. Pineapple stem extract (Bromelain) as an environmental friendly novel corrosion inhibitor for low carbon steel in 1M HCl. Measurement: Journal of the International Measurement Confederation. 134:595–605. doi:10.1016/j.measurement.2018.11.003.

Nathiya RS, Perumal S, Murugesan V, Raj V. 2019. Evaluation of extracts of Borassus flabellifer dust as green inhibitors for aluminium corrosion in acidic media. Materials Science in Semiconductor Processing. 104(July):104674. doi:10.1016/j.mssp.2019.104674.

Pradityana A, Sulistijono, Shahab A. 2013. Effectiveness of Myrmecodia Pendans extract as eco-friendly corrosion inhibitor for material API 5L grade B in 3,5% NaCl solution. Advanced Materials Research. 789:484–491. doi:10.4028/www.scientific.net/AMR.789.484.

Ramlah R, Wijaya M, Pratiwi DE. 2020. Efektivitas ekstrak daun beluntas (Pluchea indica less) sebagai inhibitor ko-

rosi pada material baja karbon dalam media NaCl 3,5%. Chemica: Jurnal Ilmiah Kimia dan Pendidikan Kimia. 21(1):86. doi:10.35580/chemica.v21i1.14843. https://ojs.unm.ac.id/chemica/article/view/14843.

Rosli NR, Yusuf SM, Sauki A, Razali WMRW. 2019. Musa sapientum (Banana) peels as green corrosion inhibitor for mild steel. Key Engineering Materials. 797:230–239. doi:10.4028/www.scientific.net/KEM.797.230.

Shi J, Ming J, Zhang Y, Jiang J. 2018. Corrosion products and corrosion-induced cracks of low-alloy steel and low-carbon steel in concrete. Cement and Concrete Composites. 88:121–129. doi:10.1016/j.cemconcomp.2018.02.002.

Susanti E, Khoirunnisa S, Mayangsari NE, Pribadi RA. 2021. Application of Borassus flabellifer lignin extract as an inhibitor of low carbon steel (LCS) corrosion rate. AIP Conference Proceedings. 2353(May). doi:10.1063/5.0052851.